

Dr. Ma Wen-Gan  
 Department of Modern Physics  
 Univ. of Sci. and Tech. of China  
 Hefei, Anhui 230027  
 P.R.China  
 Tel. (0086)-551-3606749  
 Fax. (0086)-551-3602795  
 E-mail. mawg@ustc.edu.cn

December 20, 2018

Publishing Editor  
 Journal of Physics G  
 Techno House, Redcliffe Way,  
 Bristol, BS1 6NX, England

Dear Editor,

Here we resubmit our amended manuscript named 'Single chargino production via gluon-gluon fusion in a supersymmetric theory with an explicit R-parity violation'(G/116223/PAP) by Wan Lang-Hui, Ma Wen-Gan, Yin Xi, Jiang Yi, and Han Liang to the Journal of Physics G. The responses to the suggestions and criticisms are listed below:

(1) We corrected the expressions for the sneutrino-sdown-sdown couplings in Appendix above the eq.(A.1) and recalculated the numerical results. As shown in our manuscript, the vertices of the sneutrino-sdown-sdown couplings concerned in our calculation, have the forms as(see Fig.1((b.2), Fig.1(c.2) and Eq.(A.1)):

$$V_{\tilde{\nu}_i \tilde{D}_{j,1} \bar{\tilde{D}}_{j,1}} = -i\lambda_{i,j,j}(m_{D_j} - \frac{1}{2}A_d \sin 2\theta_{D_j})$$

$$V_{\tilde{\nu}_i \tilde{D}_{j,2} \bar{\tilde{D}}_{j,2}} = -i\lambda_{i,j,j}(m_{D_j} + \frac{1}{2}A_d \sin 2\theta_{D_j})$$

where the lower indices in  $\tilde{D}_{i,k}$  refer to generation index and index of the physical squark, respectively. We find that the contribution from the trilinear soft breaking A-terms is very small. That can be understood by the following reasons. Firstly, since in above equations both A-terms in these two expressions have the opposite signs, the possible large contributions from the A-terms are canceled when we sum up the diagrams with  $\tilde{D}_{i,1}$  and  $\tilde{D}_{i,2}$

loops during our calculation. Secondly, in our numerical calculation we assumed that the mixing in the third generation sbottom-quark is very small and there are no mixings in the first and second generation sdown-quarks, respectively, therefore the contribution from large value of  $A_d$ -terms will be suppressed. We find that the discrepancy between our old and new results is very small, even we cannot distinguish the line difference in our plots.

(2) We added the sneutrino width in the definition of the sneutrino propagator  $A_{\tilde{\nu}}$  in the revised version. Actually we had included this width in our numerical calculation before. This is a misprint error.

We are very grateful for the helpful suggestions of referee.

It includes one LaTeX file and 4 eps files for figures.

With my best regards.

Sincerely yours,

Ma Wen-Gan

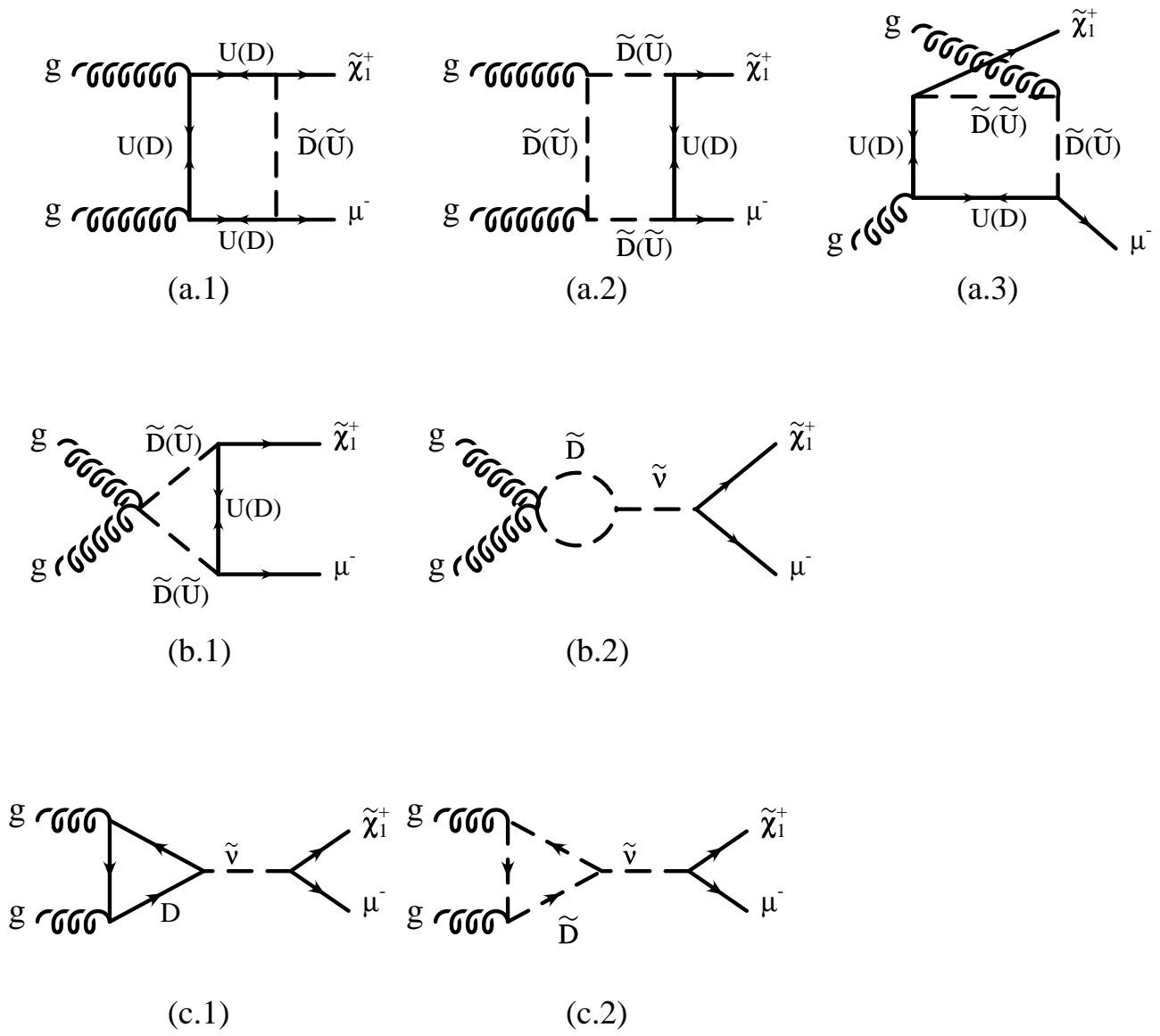


Fig.1

Fig.2

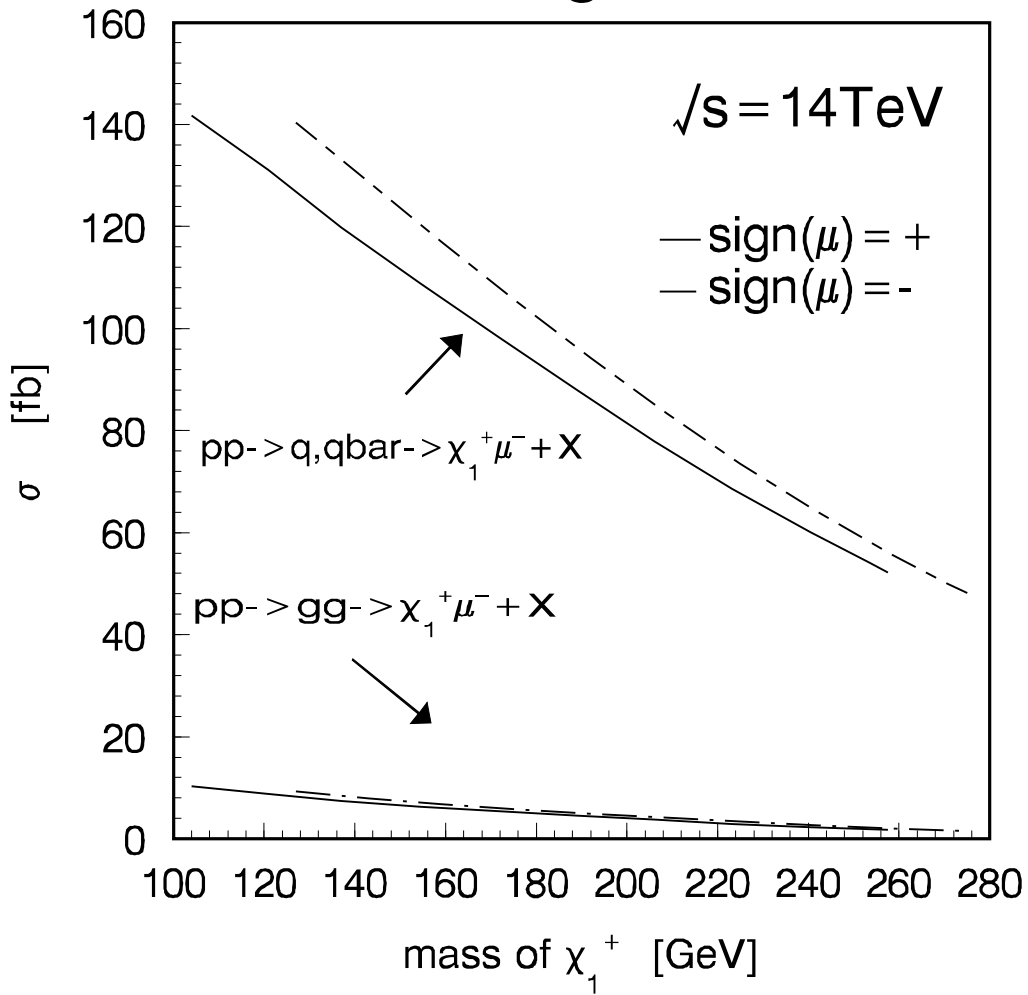


Fig.3

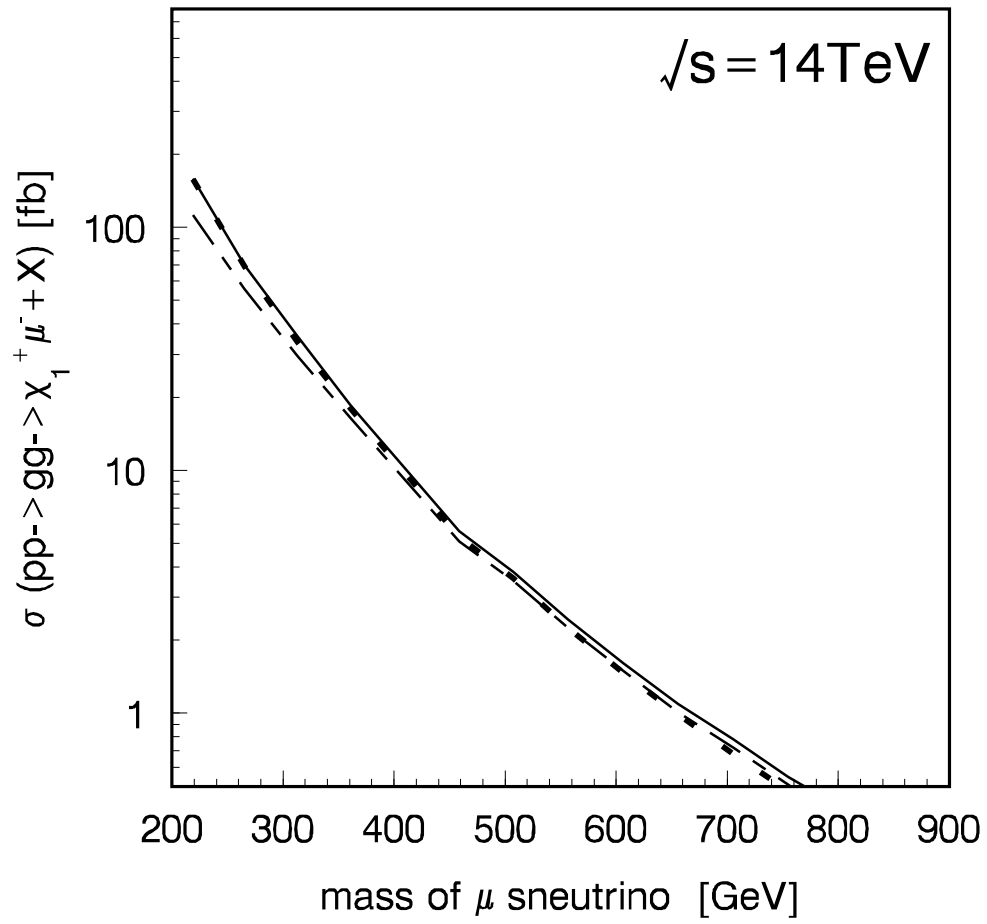
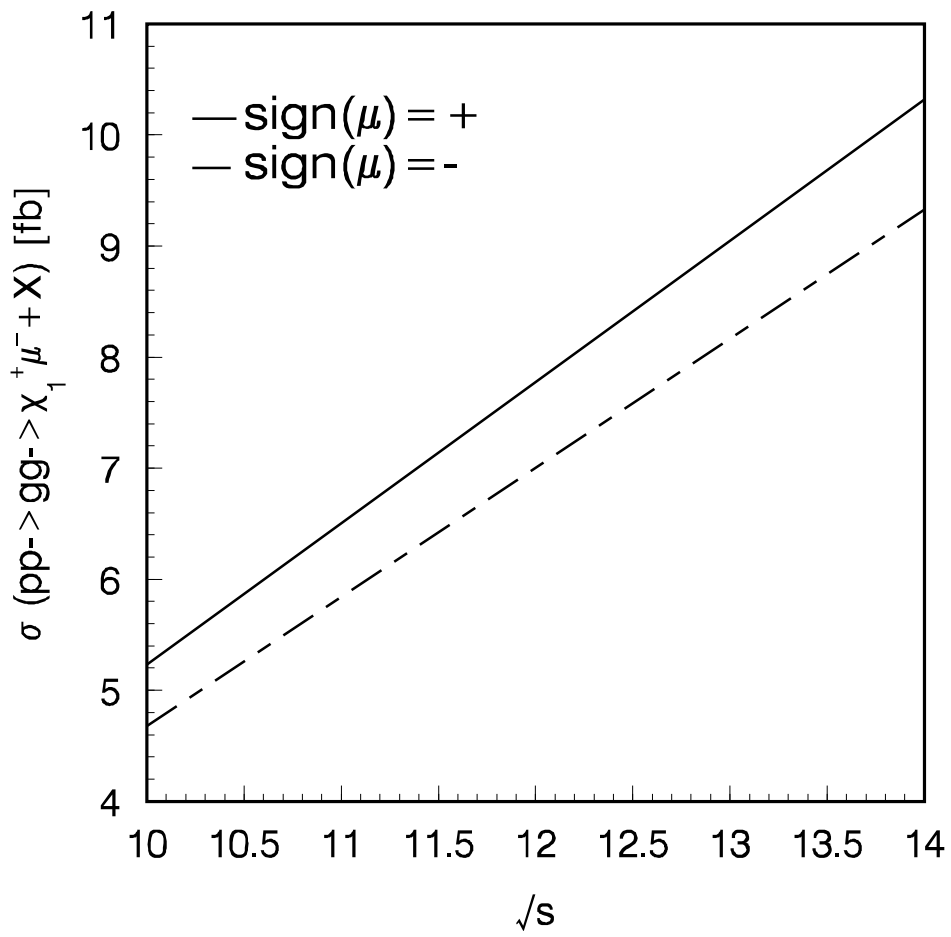


Fig.4



# Single chargino production via gluon-gluon fusion in a supersymmetric theory with an explicit R-parity violation \*

Wan Lang-Hui<sup>b</sup>, Ma Wen-Gan<sup>a,b</sup>, Yin Xi<sup>b</sup>, Jiang Yi<sup>b</sup> and Han Liang<sup>b</sup>

<sup>a</sup> CCAST (World Laboratory), P.O.Box 8730, Beijing 100080, P.R.China

<sup>b</sup> Department of Modern Physics, University of Science and Technology of China (USTC), Hefei, Anhui 230027, P.R.China

## Abstract

We studied the production of single chargino  $\tilde{\chi}_1^\pm$  accompanied by  $\mu^\mp$  lepton via gluon-gluon fusion at the LHC. The numerical analysis of their production rates is carried out in the mSUGRA scenario with some typical parameter sets. The results show that the cross sections of the  $\tilde{\chi}_1^\pm \mu^\mp$  productions via gluon-gluon collision are in the order of  $1 \sim 10^2$  femto barn quantitatively at the CERN LHC, and can be competitive with production mechanism via quark-antiquark annihilation process.

**PACS: 13.88.+e, 13.65.+i, 14.80.Dq, 14.65.-q, 14.80.Gt**

---

\*Supported by National Natural Science Foundation of China.

# I Introduction

Over the past years intensive investigations into the new physics beyond the standard model (SM) has been undertaken[1]. As the simplest extension of the SM, the supersymmetric model (SUSY) is the most attractive one. In general extended models of the SM, electroweak gauge invariance forbids terms in the SM Lagrangian that change either baryon number or lepton number, such terms are allowed in the most general supersymmetric (SUSY) extension of the SM, but they may lead to an unacceptable short proton lifetime, One way to evade the proton-decay problem is to impose a discrete symmetry conservation called R-parity ( $R_p$ ) conservation. In this case, all supersymmetric partner particles must be pair-produced, thus the lightest of superparticles must be stable.

The R-parity violation ( $R_p$ ) implies either lepton number or baryon number being broken, and it will change the feature of the SUSY models a lot. Due to the lack of experimental tests for  $R_p$  conservation, the  $R_p$  violation case is also equally well motivated in the supersymmetric extension of the SM. SUSY models with  $R_p$  can provide many interesting phenomena. Recently there are some investigations on the signal on  $R_p$  violation [2][3][4], because of experimentally observed discrepancies.

In the last few years, many efforts were made to find  $R_p$  interactions in experiments. Unfortunately, up to now we have only some upper limits on  $R_p$  parameters, such as B-violating  $R_p$  parameters ( $\lambda''$ ) and L-violating  $R_p$  parameters( $\lambda$  and  $\lambda'$ )[4][5][6] (The parameters will be defined clearly in the following sector). Therefore, trying to find the signal of  $R_p$  violation or getting more stringent constraints on the parameters in future experiments, is a promising task. The popular way to find a  $R_p$  violation signal is to



detect the decay of the lightest supersymmetric particle(LSP)[4] [6][7], but it is difficult experimentally especially at hadron colliders. The best signal for  $\tilde{R}_p$  at the CERN Large Hadron Collider (LHC) is the resonant sneutrino production through a  $\lambda'$  or a  $\lambda''$  coupling constant, respectively[8]. Because the c.m.s energy continuous distribution of the colliding partons inside protons at the hadron colliders, a intermediate resonance can be probed over a rather wide mass range. Then a single chargino can be produced by the sneutrino decays, which can be measured through the detection of its three-leptons signature.

There are two mechanisms at parton level to produce  $\tilde{\chi}_1^\pm \mu^\mp$  in an explicit R-parity violating SUSY theory at pp colliders. One is via quark and antiquark ( $q\bar{q}(q = u, d)$ ) annihilation which is allowed at tree-level. The single lightest chargino production at the LHC as induced by the resonant sneutrino production  $pp \rightarrow q\bar{q} \rightarrow \tilde{\nu}_\mu \rightarrow \tilde{\chi}_1^\pm \mu^\mp$  was studied by G. Moreau et.al.[8]. Another mechanism is via gluon-gluon fusion. The single lightest chargino production process via gluon-gluon fusion, which will take place at the lowest order by one-loop diagrams, could be also significant due to large gluon luminosity in distribution function of proton.

In this paper, we investigate the resonant sneutrino particle production via gluon-gluon fusion at the LHC operating at the energy of 14  $TeV$ . We arrange this paper as follows. In Sec.II we present the analytical calculations of both subprocess and parent process. In Sec.III we give some numerical presentations in the MSSM and the minimal supergravity (mSUGRA) scenario [9], and discuss these numerical results. The conclusions are contained in Sec.IV. Finally some notations used in this paper, the explicit expressions of the form factors induced by the loop diagrams are collected in Appendix.

## II The Calculation of $pp \rightarrow gg \rightarrow \tilde{\chi}_1^\pm \mu^\mp + X$

The R-parity of a particle is defined as  $R_p = (-1)^{2S+3B+L}$  [10], where  $S$  is the spin quantum number of the particle,  $L$  the lepton number and  $B$  the baryon number. The minimal supersymmetric model (MSSM) does not contain the most general superpotential respecting to the gauge symmetries of the SM, which includes bilinear and trilinear terms, which can be expressed as

$$W_{\not{R}_p} = \frac{1}{2} \lambda_{[ij]k} L_i \cdot L_j \bar{E}_k + \lambda'_{ijk} L_i \cdot Q_j \bar{D}_k + \frac{1}{2} \lambda''_{i[jk]} \bar{U}_i \bar{D}_j \bar{D}_k + \epsilon_i L_i H_u. \quad (2.1)$$

where  $L_i, Q_i$  are the SU(2) doublet lepton and quark fields,  $E_i, U_i, D_i$  are the singlet superfields. The  $UDD$  couplings violate baryon number while the other three sets violate lepton number. We shall explicitly forbid the  $UDD$  interactions as an economical way to avoid unacceptable rapid proton decay[11], and the term of  $LLE$  have no contribution to our process  $pp \rightarrow gg \rightarrow \tilde{\chi}_1^\pm \mu^\mp + X$ , we shall not discuss them too. In this work we ignored the bilinear terms that mix lepton and Higgs superfields [3] for simplicity, because its effects are small in our process.

Expanding the superfield components in Eq.(2.1) we obtain the interaction Lagrangian that contains quarks and leptons:

$$\mathcal{L}_{LQD} = \lambda'_{ijk} \{ \tilde{\nu}_{iL} \bar{d}_{kR} d_{jL} - \tilde{e}_{iL} \bar{d}_{kR} u_{jL} + \tilde{d}_{jL} \bar{d}_{kR} \nu_{iL} - \tilde{u}_{jL} \bar{d}_{kR} e_{iL} + \tilde{d}_{kR}^c \nu_{iL} d_{jL} - \tilde{d}_{kR}^c e_{iL} u_{jL} \} + h.c. \quad (2.2)$$

The subprocess  $gg \rightarrow \tilde{\chi}_1^\pm \mu^\mp$  can only be produced through one-loop diagram in the lowest order. In this case it is not necessary to consider the renormalization. The generic Feynman diagrams contributing to the subprocess in the MSSM without R-parity at one-

loop level are depicted in Fig.1, where the exchange of incoming gluons in Fig.1(a.1 ~ 3) and Fig.1(c.1,2) are not shown. We divide all the one-loop diagrams in Fig.1 into three groups: (1) box diagrams shown in Fig.1(a), (2) quartic interaction diagrams in Fig.1(b), (3) triangle diagrams shown in Fig.1(c). In this work, we perform the calculation in the 't Hooft-Feynman gauge. The relevant Feynman rules without  $R_p$  interactions can be found in references[1] [12][13]. The related Feynman rules with  $R_p$  interactions can be read out from Eq.(2.2).

If we ignore the CP violation, the cross section of  $pp \rightarrow gg \rightarrow \tilde{\chi}_1^+ \mu^- + X$  coincides with the process  $pp \rightarrow gg \rightarrow \tilde{\chi}_1^- \mu^+$  because of charge conjugation invariance and we shall specify on the calculation of the  $\tilde{\chi}_1^+ \mu^-$  production for simplicity in the following. We denote the reaction of  $\tilde{\chi}_1^+$  and  $\mu^-$  production via gluon-gluon fusion as:

$$g(p_1, \alpha, \mu)g(p_2, \beta, \nu) \longrightarrow \tilde{\chi}_1^+(k_1)\mu^-(k_2). \quad (2.3)$$

where  $p_1$  and  $p_2$  denote the four momenta of the incoming gluons,  $k_1, k_2$  denote the four momenta of the outgoing chargino and  $\mu^-$  lepton respectively, and  $\alpha, \beta$  are color indices of the colliding gluons.

The corresponding matrix element of Feynman diagrams in Fig.1, can be written as

$$\begin{aligned} \mathcal{M} = & \mathcal{M}^b + \mathcal{M}^q + \mathcal{M}^{tr} = \epsilon^\mu(p_1)\epsilon^\nu(p_2)\bar{u}(k_1)\{f_1g_{\mu\nu} + f_2g_{\mu\nu}\gamma_5 + f_3k_{1\mu}k_{1\nu} + f_4k_{1\mu}k_{1\nu}\gamma_5 \\ & + f_5k_{1\nu}\gamma_\mu + f_6k_{1\mu}\gamma_\nu + f_7g_{\mu\nu}\not{p}_1 + f_8k_{1\mu}k_{1\nu}\not{p}_1 + f_9g_{\mu\nu}\not{p}_2 + f_{10}k_{1\mu}k_{1\nu}\not{p}_2 + f_{11}k_{1\nu}\gamma_5\gamma_\mu \\ & + f_{12}k_{1\mu}\gamma_5\gamma_\nu + f_{13}g_{\mu\nu}\gamma_5\not{p}_1 + f_{14}k_{1\mu}k_{1\nu}\gamma_5\not{p}_1 + f_{15}g_{\mu\nu}\gamma_5\not{p}_2 + f_{16}k_{1\mu}k_{1\nu}\gamma_5\not{p}_2 \\ & + f_{17}k_{1\nu}\gamma_\mu\not{p}_1 + f_{18}k_{1\nu}\gamma_5\gamma_\mu\not{p}_1 + f_{19}\gamma_\mu\gamma_\nu\not{p}_1 + f_{20}k_{1\nu}\gamma_\mu\not{p}_1\not{p}_2 + f_{21}\gamma_5\gamma_\mu\gamma_\nu\not{p}_1 \\ & + f_{22}k_{1\nu}\gamma_5\gamma_\mu\not{p}_1\not{p}_2 + f_{23}k_{1\mu}\gamma_\nu\not{p}_2 + f_{24}k_{1\mu}\gamma_5\gamma_\nu\not{p}_2 + f_{25}\gamma_\mu\gamma_\nu\not{p}_2 + f_{26}k_{1\mu}\gamma_\nu\not{p}_1\not{p}_2 \end{aligned}$$

$$\begin{aligned}
& + f_{27}\gamma_5\gamma_\mu\gamma_\nu\not{p}_2 + f_{28}k_{1\mu}\gamma_5\gamma_\nu\not{p}_1\not{p}_2 + f_{29}\epsilon_{\mu\nu\alpha\beta}p_1^\alpha p_2^\beta + f_{30}\epsilon_{\mu\nu\alpha\beta}p_1^\alpha p_2^\beta\gamma_5 + f_{31}\gamma_\mu\gamma_\nu \\
& + f_{32}\gamma_5\gamma_\mu\gamma_\nu + f_{33}\gamma_\mu\gamma_\nu\not{p}_1\not{p}_2 + f_{34}\gamma_5\gamma_\mu\gamma_\nu\not{p}_1\not{p}_2 + f_{35}g_{\mu\nu}\not{p}_1\not{p}_2 + f_{36}g_{\mu\nu}\gamma_5\not{p}_1\not{p}_2\}v(k_2)
\end{aligned}$$

where  $\mathcal{M}^b$ ,  $\mathcal{M}^q$ , and  $\mathcal{M}^{tr}$  are the matrix elements contributed by box, quartic and triangle interaction diagrams, respectively. The cross section for this subprocess at one loop order in unpolarized gluon collisions can be obtained by

$$\hat{\sigma}(\hat{s}, gg \rightarrow \tilde{\chi}_1^+ \mu^-) = \frac{1}{16\pi\hat{s}^2} \int_{\hat{t}^-}^{\hat{t}^+} d\hat{t} \sum_{\bar{}} |\mathcal{M}|^2. \quad (2.4)$$

In above equation,  $\hat{t}$  is the momentum transfer squared from one of the incoming gluons to the charged boson in the final state, and

$$\hat{t}^\pm = \frac{1}{2} \left[ (m_{\tilde{\chi}_1^+}^2 + m_\mu^2 - \hat{s}) \pm \sqrt{(m_{\tilde{\chi}_1^+}^2 + m_\mu^2 - \hat{s})^2 - 4m_{\tilde{\chi}_1^+}^2 m_\mu^2} \right].$$

The bar over the sum means average over initial spin and color.

With the results from Eq.(2.4), we can easily obtain the total cross section at  $pp$  collider by folding the cross section of subprocess  $\hat{\sigma}(gg \rightarrow \tilde{\chi}_1^+ \mu^-)$  with the gluon luminosity.

$$\sigma(s, pp \rightarrow gg \rightarrow \tilde{\chi}_1^+ \mu^- + X) = \int_{(m_{\tilde{\chi}_1^+}^2 + m_\mu^2)/s}^1 d\tau \frac{d\mathcal{L}_{gg}}{d\tau} \hat{\sigma}(gg \rightarrow \tilde{\chi}_1^+ \mu^- \text{ at } \hat{s} = \tau s), \quad (2.5)$$

where  $\sqrt{s}$  and  $\sqrt{\hat{s}}$  are the  $pp$  and  $gg$  c.m.s. energies respectively and  $d\mathcal{L}_{gg}/d\tau$  is the distribution function of gluon luminosity, which is defined as

$$\frac{d\mathcal{L}_{gg}}{d\tau} = \int_\tau^1 \frac{dx_1}{x_1} \left[ f_g(x_1, Q^2) f_g\left(\frac{\tau}{x_1}, Q^2\right) \right]. \quad (2.6)$$

here  $\tau = x_1 x_2$ , the definition of  $x_1$  and  $x_2$  are from [14], and in our calculation we adopt the MRS set G parton distribution function [15]. The factorization scale  $Q$  was chosen as the average of the final particles masses  $\frac{1}{2}(m_{\tilde{\chi}_1^+} + m_\mu)$ .

### III Numerical results and discussions

In this section, we present some numerical results of the total cross section from the complete one-loop diagrams for the processes  $pp \rightarrow gg \rightarrow \tilde{\chi}_1^+ \mu^-$ . In our numerical calculation to get the low energy scenario from the mSUGRA[9], the complete 2-loop renormalisation group equations(RGE's) of the superpotential parameters for the supersymmetric standard model including the full set of R-parity violating couplings have been obtained in [16], here we neglect the effects of R-parity violation in the RGE's for simplicity. The RGE's (RGE's)[17] are run from the weak scale  $m_Z$  up to the GUT scale, taking all thresholds into account. We use two loop RGE's only for the gauge couplings and the one-loop RGE's for the other supersymmetric parameters. The GUT scale boundary conditions are imposed and the RGE's are run back to  $m_Z$ , again taking threshold into account. We chose  $R_p$ -Parity violating parameters concerned in the subprocess via gluon-gluon fusion to be  $\lambda'_{211} = 0.05$ ,  $\lambda'_{222} = 0.21$  and  $\lambda'_{233} = 0.3$ , which satisfy the constraints given by [18]. The SM input parameters are chosen as:  $m_t = 173.8 \text{ GeV}$ ,  $m_Z = 91.187 \text{ GeV}$ ,  $m_b = 4.5 \text{ GeV}$ ,  $\sin^2 \theta_W = 0.2315$ , and  $\alpha_{EW} = 1/128$ . We take a simple one-loop formula for the running strong coupling constant  $\alpha_s$ .

$$\alpha_s(\mu) = \frac{\alpha_s(m_Z)}{1 + \frac{33-2n_f}{6\pi} \alpha_s(m_Z) \ln \frac{\mu}{m_Z}}. \quad (3.1)$$

where  $\alpha_s(m_Z) = 0.117$  and  $n_f$  is the number of active flavors at energy scale  $\mu$ .

The cross sections for  $\tilde{\chi}_1^+ \mu^-$  via  $gg$  collisions at hadron colliders versus the mass of  $\tilde{\chi}_1^+$  is shown in Fig.2. The input parameters are chosen as  $m_0 = 400 \text{ GeV}$ ,  $A_0 = 300 \text{ GeV}$ ,

$\tan \beta = 4$ , and  $m_{1/2}$  varies from  $150 \text{ GeV}$  to  $330 \text{ GeV}$ . With above chosen parameters, we get that the value of  $m_{\tilde{\chi}_1^+}$  varies from  $104 \text{ GeV}$  to  $270 \text{ GeV}$  in the framework of the mSUGRA as shown in Fig.2. We calculate the cross sections at the LHC with the energies of  $\sqrt{s}$  being  $14 \text{ TeV}$ . For the comparison, we also present the cross section of  $\tilde{\chi}_1^+ \mu^-$  via quark-antiquark with the same input parameters in Fig.2. It shows the cross section contribution to parent process at hadron collider from subprocess  $gg \rightarrow \tilde{\chi}_1^+ \mu^-$  can be competitive with that via  $q\bar{q}$  annihilation. Then the production mechanism of subprocess  $gg \rightarrow \tilde{\chi}_1^+ \mu^-$  should be considered in detecting the  $R_p$  signals in this parameter space. We can see from Fig.2 that the cross sections for  $pp \rightarrow gg \rightarrow \tilde{\chi}_1^+ \mu^-$  decreases with the increment of the mass of  $\tilde{\chi}_1^+$ . It can reach 10.3 femto barn when  $m_{\tilde{\chi}_1^+}$  is about  $104 \text{ GeV}$ .

In Fig.3 we present the cross sections of  $\tilde{\chi}_1^+ \mu^-$  productions versus the mass of  $\mu$  sneutrino with the collision energy of hadron being  $14 \text{ TeV}$ , where the input parameters are chosen as  $m_{1/2} = 150 \text{ GeV}$ ,  $A_0 = 300 \text{ GeV}$  and  $\tan \beta = 4$ . In the mSUGRA scenario, when  $m_0$  increases from  $200 \text{ GeV}$  to  $800 \text{ GeV}$ , the mass of  $\mu$  sneutrino ranges from  $219 \text{ GeV}$  to  $804 \text{ GeV}$ . We can see from Fig.3 that the cross section decreases rapidly with the increment of the mass of  $\mu$  sneutrino, this is because the cross section is enhanced by the  $\mu$  sneutrino resonance effects in the lower  $\mu$  sneutrino mass range. We also show the cross section contributed by the  $\hat{s}$  channel diagrams. It shows that the cross section are mostly contributed by the effects of resonance, only when the mass of  $\mu$  sneutrino is larger than  $700 \text{ GeV}$ , the non-resonant contributions can reach about 15% to the total cross sections.

The cross sections for the production of single chargino accompanied by  $\mu$  lepton via gluon-gluon versus  $\sqrt{s}$  with  $m_{1/2} = 150 \text{ GeV}$ ,  $m_0 = 400 \text{ GeV}$ ,  $A_0 = 300 \text{ GeV}$ ,  $\tan \beta=4$

are depicted in Fig.4. The solid line is for  $\mu > 0$ , and the dashed line is for  $\mu < 0$ . The discrepancy between these two curves is not very large. This feature can be seen also in the corresponding curves in Fig.2 and Fig.3. It shows that the production rate of process  $pp \rightarrow gg \rightarrow \tilde{\chi}_1^\pm \mu^\mp + X$  is not very sensitive to the sign of parameter  $\mu$ .

Finally, we will discuss the relationship between the cross section and the parameter  $\lambda'_{ijk}$ . The cross section of  $\tilde{\chi}_1^+ \mu^-$  production via  $q\bar{q}$  annihilation is scaled by  $\lambda_{211}^{\prime 2}$ . While the cross section via  $gg$  should take the sum of three generation of (s)quarks loop, but the main contribution to the cross section is from the third generation for the coupling coefficient of the third generation is much larger than the first and second generation, then the cross section is nearly proportional to the  $\lambda_{233}^{\prime 2}$ . If  $\lambda_{233}'$  is less than 0.18, The cross section via  $gg$  will be less than 3.5 femto barn, in this case, compared with the process of  $q\bar{q}$  annihilation, it can be neglected. But if  $\lambda_{233}'$  is larger than the value we discussed, the process via  $gg$  will play a more important rule in  $pp$  collision. In fact, the maximal possible cross section could be somewhat higher than indicated in fig.3, because the upper bounds of R-parity violation couplings can be higher for heavy sparticls.

## IV Summary

In this paper, we have studied the production of single chargino  $\tilde{\chi}_1^\pm$  associated with  $\mu$  lepton with explicit  $R_p$ -violation at hadron colliders. The production rates via gluon-gluon fusion at the LHC are numerically analysed in the mSUGRA scenario with some typical parameter sets. The results show that the cross section of the  $\tilde{\chi}_1^\pm \mu^\mp$  production via gluon-gluon collisions can reach about some femto barn to hundreds femto barn at

the LHC with our chosen parameters. It shows that the production mechanism via gluon-gluon fusion can be competitive with that from quark-antiquark annihilation process. Therefore, In detecting the  $\tilde{\chi}_1^\pm \mu^\mp$  productions at the LHC to search for the signals of both SUSY and  $R_p$  violation, we should consider not only the  $\tilde{\chi}_1^\pm \mu^\mp$  production subprocesses via quark-antiquark annihilation, but also those via the gluon-gluon fusion.

**Acknowledgement:** This work was supported in part by the National Natural Science Foundation of China(project number: 19875049), the Youth Science Foundation of the University of Science and Technology of China, a grant from the Education Ministry of China and the State Commission of Science and Technology of China.

One of the author Wan Lang-Hui would thank Zhou Mian-Lai, Zhou Fei and Zhou Hong for useful discussion.

## Appendix

The Feynman rules for the couplings we used are list below:

$$\begin{aligned}
\bar{U}_n - \tilde{D}_{n,i} - \tilde{\chi}_j^+ &: V_{U_n \tilde{D}_{n,i} \tilde{\chi}_j^+}^{(1)} P_L + V_{U_n \tilde{D}_{n,i} \tilde{\chi}_j^+}^{(2)} P_R, \\
\bar{D}_n - \tilde{U}_{n,i} - \tilde{\chi}_j^{+c} &: \{V_{D_n \tilde{U}_{n,i} \tilde{\chi}_j^+}^{(1)} P_L + V_{D_n \tilde{U}_{n,i} \tilde{\chi}_j^+}^{(2)} P_R\} C, \\
\bar{E}_n - \tilde{\nu}_{E_n} - \tilde{\chi}_j^{+c} &: \{V_{E_n \tilde{\nu}_{E_n} \tilde{\chi}_j^+}^{(1)} P_L + V_{E_n \tilde{\nu}_{E_n} \tilde{\chi}_j^+}^{(2)} P_R\} C, \\
\tilde{\nu}_i - D_j - \bar{D}_k &: V_{\tilde{\nu}_i D_j D_k}^{(1)} P_L + V_{\tilde{\nu}_i D_j D_k}^{(2)} P_R \\
\bar{E}_i - D_j - \tilde{U}_{k,n} &: V_{E_i D_j \tilde{U}_{k,n}}^{(2)} P_R \\
E_i^c - \bar{U}_j - \tilde{D}_{k,n} &: V_{E_i U_j \tilde{D}_{k,n}}^{(2)} P_R C \\
\tilde{\nu}_i - \tilde{D}_{j,l} - \tilde{\bar{D}}_{k,n} &: V_{\tilde{\nu}_i \tilde{D}_{j,l} \tilde{\bar{D}}_{k,n}}
\end{aligned}$$



Where  $C$  is the charge conjugation operator,  $P_{L,R} = \frac{1}{2}(1 \mp \gamma_5)$ . The lower-index in  $Q_i(E_i)$  refers to the generation index of quarks and leptons, the lower-indices in  $\tilde{Q}_{i,j}$  ( $Q = U, D$ ) represent generation index and index of the physical squark, respectively. For the expressions of  $V_{U_n \tilde{D}_{n,i} \tilde{\chi}_j^+}^{(1,2)}$  and  $V_{D_n \tilde{U}_{n,i} \tilde{\chi}_j^+}^{(1,2)}$ , one can refer Ref.[13], the forms of  $V_{E_n \tilde{\nu}_{E_n} \tilde{\chi}_j^+}^{(1,2)}$  can be found in Ref.[1]. The other vertices can be read out from Eq.(2.2):

$$V_{\tilde{\nu}_i D_j D_k}^{(1)} = -i\lambda'_{ijk}, \quad V_{\tilde{\nu}_i D_j D_k}^{(2)} = -i\lambda'_{ikj}$$

$$V_{E_i D_j \tilde{U}_{k,1}}^{(2)} = i\lambda'_{ijk} \cos \theta_{U_k}, \quad V_{E_i D_j \tilde{U}_{k,2}}^{(2)} = i\lambda'_{ijk} \sin \theta_{U_k},$$

$$V_{E_i U_j \tilde{D}_{k,1}}^{(2)} = -i\lambda'_{ijk} \sin \theta_{D_k}, \quad V_{E_i U_j \tilde{D}_{k,2}}^{(2)} = i\lambda'_{ijk} \cos \theta_{D_k}.$$

$$V_{\tilde{\nu}_i \tilde{D}_{j,1} \tilde{D}_{k,1}} = -i\lambda'_{ijk} \left[ m_{D_j} \sin \theta_{D_j} \sin \theta_{D_k} + m_{D_k} \cos \theta_{D_j} \cos \theta_{D_k} - A_d \cos \theta_{D_j} \sin \theta_{D_k} \right].$$

$$V_{\tilde{\nu}_i \tilde{D}_{j,2} \tilde{D}_{k,2}} = -i\lambda'_{ijk} \left[ m_{D_j} \cos \theta_{D_j} \cos \theta_{D_k} + m_{D_k} \sin \theta_{D_j} \sin \theta_{D_k} + A_d \sin \theta_{D_j} \cos \theta_{D_k} \right].$$

where  $A_d$  is the soft breaking parameter. The amplitude parts for the  $u$ -channel box and triangle vertex interaction diagrams can be obtained from the  $t$ -channel's by doing exchanges as shown below:

$$\mathcal{M}^{\hat{u}} = \mathcal{M}^{\hat{t}}(\hat{t} \rightarrow \hat{u}, k_1 \leftrightarrow k_2, \mu \leftrightarrow \nu), \quad (\text{A.1})$$

So we present only the  $t$ -channel form factors for box and triangle diagrams. The form factors for the figures with loop of  $U$  quark and  $\tilde{D}$  squark in Fig.1(a,b), can be obtained from the form factors corresponding to the figures with loop of  $D$  quark and  $\tilde{U}$  squark in Fig.1(a.1), (b.1) by doing the replacement of  $m_D \rightarrow m_U$ ,  $m_{\tilde{U}_{j,k}} \rightarrow m_{\tilde{D}_{j,k}}$ ,  $F_{1,k} \rightarrow F_{3,k}$ ,  $F_{2,k} \rightarrow F_{4,k}$ ,  $C^{1,k} \rightarrow C^{3,k}$ ,  $D^{1,k} \rightarrow D^{4,k}$ ,  $D^{2,k} \rightarrow D^{5,k}$  and  $D^{3,k} \rightarrow D^{6,k}$ . Since the form factors of figures with the first or second generation quark and squark

loop are analogous to corresponding ones with the third generation quark and squark loop, here we give only the form factors for the figures in Fig.1(a),(b) including the third generation quark and squark loop. In this appendix, we use the notations defined below for abbreviation:

$$B_0 = B_0[-p_1, m_b, m_b]$$

$$B_0^1 = B_0[\hat{s}, m_{\tilde{b}_k}, m_{\tilde{b}_k}]$$

$$C_0^{1,k}, C_{ij}^{1,k} = C_0, C_{ij}[k_2, k_1, m_{\tilde{t}_k}, m_b, m_{\tilde{t}_k}]$$

$$C_0^2 = C_0[-p_1, -p_2, m_b, m_b, m_b]$$

$$C_0^{3,k}, C_{ij}^{3,k} = C_0, C_{ij}[k_2, k_1, m_{\tilde{b}_k}, m_t, m_{\tilde{b}_k}]$$

$$C_0^4, C_{ij}^4 = C_0, C_{ij}[-p_2, -p_1, m_b, m_b, m_b]$$

$$C_0^{5,k}, C_{ij}^{5,k} = C_0, C_{ij}[-p_2, -p_1, m_{\tilde{b}_k}, m_{\tilde{b}_k}, m_{\tilde{b}_k}]$$

$$D_0^{1,k}, D_{ij}^{1,k}, D_{ijl}^{1,k} = D_0, D_{ij}, D_{ijl}[-p_2, k_1, -p_1, m_{\tilde{t}_k}, m_{\tilde{t}_k}, m_b, m_b]$$

$$D_0^{2,k}, D_{ij}^{2,k}, D_{ijl}^{2,k} = D_0, D_{ij}, D_{ijl}[k_1, -p_1, -p_2, m_{\tilde{t}_k}, m_b, m_b, m_b]$$

$$D_0^{3,k}, D_{ij}^{3,k}, D_{ijl}^{3,k} = D_0, D_{ij}, D_{ijl}[k_1, -p_1, -p_2, m_b, m_{\tilde{t}_k}, m_{\tilde{t}_k}, m_{\tilde{t}_k}]$$

$$D_0^{4,k}, D_{ij}^{4,k}, D_{ijl}^{4,k} = D_0, D_{ij}, D_{ijl}[-p_2, k_1, -p_1, m_{\tilde{b}_k}, m_{\tilde{b}_k}, m_t, m_t]$$

$$D_0^{5,k}, D_{ij}^{5,k}, D_{ijl}^{5,k} = D_0, D_{ij}, D_{ijl}[k_1, -p_1, -p_2, m_{\tilde{b}_k}, m_t, m_t, m_t]$$

$$D_0^{6,k}, D_{ij}^{6,k}, D_{ijl}^{6,k} = D_0, D_{ij}, D_{ijl}[k_1, -p_1, -p_2, m_t, m_{\tilde{b}_k}, m_{\tilde{b}_k}, m_{\tilde{b}_k}]$$

$$A_{\tilde{\nu}} = \frac{i}{\hat{s} - m_{\tilde{\nu}_\mu}^2 + im_{\tilde{\nu}_\mu}\Gamma_{\tilde{\nu}_\mu}}$$

$$F_{1,k} = V_{\mu b \tilde{t}_k}^{(2)} V_{b \tilde{t}_k \tilde{\chi}_1^+}^{(1)}$$

$$F_{2,k} = V_{\mu b \tilde{t}_k}^{(2)} V_{b \tilde{t}_k \tilde{\chi}_1^+}^{(2)}$$

$$F_{3,k} = V_{i\tilde{b}_k\tilde{\chi}_1^+}^{(2)*} V_{\mu t\tilde{b}_k}^{(2)}$$

$$F_{4,k} = V_{i\tilde{b}_k\tilde{\chi}_1^+}^{(1)*} V_{\mu t\tilde{b}_k}^{(2)}$$

The form factors in the amplitude of the quartic interaction diagrams Fig.1(b) and are expressed as

$$f_1^q = \frac{ig_s^2}{32\pi^2} \sum_{k=1}^2 (C_0^{1,k} F_{2,k} m_b - C_{12}^{1,k} F_{1,k} m_{\tilde{\chi}_1^+} + (C_0^{1,k} + C_{11}^{1,k}) F_{1,k} m_\mu + B_0^1 V_{\tilde{\nu}_\mu \tilde{b}_k \tilde{b}_k}^* A_{\tilde{\nu}} V_{\mu \tilde{\nu}_\mu \tilde{\chi}_1^+}^{(2)})$$

$$f_2^q = \frac{ig_s^2}{32\pi^2} \sum_{k=1}^2 (C_0^{1,k} F_{2,k} m_b - C_{12}^{1,k} F_{1,k} m_{\tilde{\chi}_1^+} - (C_0^{1,k} + C_{11}^{1,k}) F_{1,k} m_\mu + B_0^1 V_{\tilde{\nu}_\mu \tilde{b}_k \tilde{b}_k}^* A_{\tilde{\nu}} V_{\mu \tilde{\nu}_\mu \tilde{\chi}_1^+}^{(2)})$$

$$f_i^q = 0 \quad (i = 3 - 36)$$

The form factors in the amplitude from the  $t$ -channel triangle diagrams depicted in fig.1(c) are list below:

$$f_1^{tr} = f_2^{tr} = -\frac{g_S^2}{64\pi^2} (2B_0 - 8C_{24}^4 - C_0^4 - 2C_{12}^4 s) m_b A_{\tilde{\nu}} (V_{\tilde{\nu}_\mu b b}^{(1)*} + V_{\tilde{\nu}_\mu b b}^{(2)*}) V_{\mu \tilde{\nu}_\mu \tilde{\chi}_1^+}^{(2)}$$

$$- \frac{ig_s^2}{16\pi^2} \sum_{k=1}^2 C_{24}^{5,k} V_{\tilde{\nu}_\mu \tilde{b}_k \tilde{b}_k}^* A_{\tilde{\nu}} V_{\mu \tilde{\nu}_\mu \tilde{\chi}_1^+}^{(2)}$$

$$f_i^{tr} = 0 \quad (i = 3 - 36)$$

The form factors of the amplitude part from  $t$ -channel box diagrams, Fig.1 (a) are written as

$$f_1^{b,t} = f_2^{b,t} = -\frac{ig_s^2}{16\pi^2} \sum_{k=1}^2 \left[ (D_{27}^{1,k} + D_{27}^{2,k} + D_{27}^{3,k}) F_{2,k} m_b \right. \\ \left. + (D_{27}^{1,k} + D_{312}^{1,k} + D_{27}^{2,k} + D_{311}^{2,k} - D_{311}^{3,k}) F_{1,k} m_{\tilde{\chi}_1^+} \right]$$

$$f_3^{b,t} = f_4^{b,t} = \frac{ig_s^2}{16\pi^2} \sum_{k=1}^2 \left[ (D_{12}^{1,k} + D_{22}^{1,k} + D_0^{2,k} + 2D_{11}^{2,k} + D_{21}^{2,k} + D_0^{3,k} + 2D_{11}^{3,k} + D_{21}^{3,k}) F_{2,k} m_b \right. \\ \left. + (D_{12}^{1,k} + 2D_{22}^{1,k} + D_{32}^{1,k} + D_0^{2,k} + 3D_{11}^{2,k} + 3D_{21}^{2,k} + D_{31}^{2,k} - D_{11}^{3,k} - 2D_{21}^{3,k} - D_{31}^{3,k}) F_{1,k} m_{\tilde{\chi}_1^+} \right]$$

$$f_5^{b,t} = \frac{ig_s^2}{32\pi^2} \sum_{k=1}^2 F_{1,k} \left[ 2D_{27}^{1,k} + 4D_{312}^{1,k} - D_{12}^{1,k} \hat{s} - D_{24}^{1,k} \hat{s} - D_{26}^{1,k} \hat{s} - D_{310}^{1,k} \hat{s} - D_{26}^{1,k} \hat{t} \right]$$

$$\begin{aligned}
& - D_{38}^{1,k} \hat{t} + 4D_{27}^{2,k} + 4D_{311}^{2,k} - D_{13}^{2,k} \hat{s} - D_{25}^{2,k} \hat{s} - D_{26}^{2,k} \hat{s} - D_{310}^{2,k} \hat{s} - D_{12}^{2,k} \hat{t} - 2D_{24}^{2,k} \hat{t} \\
& - D_{12}^{1,k} \hat{u} - D_{22}^{1,k} \hat{u} - D_{24}^{1,k} \hat{u} - D_{36}^{1,k} \hat{u} + D_{12}^{1,k} m_b^2 - D_{34}^{2,k} \hat{t} - D_{13}^{2,k} \hat{u} - 2D_{25}^{2,k} \hat{u} - D_{35}^{2,k} \hat{u} \\
& + (D_0^{2,k} + D_{11}^{2,k}) m_b^2 + 2D_{27}^{3,k} + 2D_{311}^{3,k} + (D_{13}^{2,k} - D_0^{2,k} - 3D_{11}^{2,k} + D_{12}^{2,k} - 3D_{21}^{2,k} + 2D_{24}^{2,k} \\
& + 2D_{25}^{2,k} - D_{31}^{2,k} + D_{34}^{2,k} + D_{35}^{2,k} + D_{24}^{1,k} - D_{22}^{1,k} + D_{26}^{1,k} - D_{32}^{1,k} + D_{36}^{1,k} + D_{38}^{1,k}) m_{\tilde{\chi}_1^+}^2 \\
f_6^{b,t} &= -\frac{ig_s^2}{32\pi^2} \sum_{k=1}^2 F_{1,k} \left[ 2D_{27}^{1,k} + 2D_{312}^{1,k} + C_0^2 - 2D_{27}^{2,k} + 2D_{311}^{2,k} + D_{26}^{2,k} \hat{s} + D_{24}^{2,k} \hat{t} + D_{25}^{2,k} \hat{u} \right. \\
& \left. - 2D_{27}^{3,k} - 2D_{311}^{3,k} + (D_{21}^{2,k} - D_{24}^{2,k} - D_{25}^{2,k}) m_{\tilde{\chi}_1^+}^2 - D_0^{2,k} m_{t_k}^2 \right] \\
f_7^{b,t} &= \frac{ig_s^2}{16\pi^2} \sum_{k=1}^2 F_{1,k} \left[ D_{27}^{1,k} + D_{313}^{1,k} + D_{27}^{2,k} + D_{312}^{2,k} - D_{312}^{3,k} \right] \\
f_8^{b,t} &= -\frac{ig_s^2}{16\pi^2} \sum_{k=1}^2 F_{1,k} \left[ D_{26}^{1,k} + D_{38}^{1,k} + D_{12}^{2,k} + 2D_{24}^{2,k} + D_{34}^{2,k} - D_{12}^{3,k} - 2D_{24}^{3,k} - D_{34}^{3,k} \right] \\
f_9^{b,t} &= \frac{ig_s^2}{16\pi^2} \sum_{k=1}^2 F_{1,k} \left[ D_{27}^{1,k} + D_{311}^{1,k} + D_{313}^{2,k} - D_{313}^{3,k} \right] \\
f_{10}^{b,t} &= -\frac{ig_s^2}{16\pi^2} \sum_{k=1}^2 F_{1,k} \left[ D_{12}^{1,k} + D_{22}^{1,k} + D_{24}^{1,k} + D_{36}^{1,k} + D_{13}^{2,k} + 2D_{25}^{2,k} + D_{35}^{2,k} \right. \\
& \left. - D_{13}^{3,k} - 2D_{25}^{3,k} - D_{35}^{3,k} \right] \\
f_{11}^{b,t} &= -\frac{ig_s^2}{32\pi^2} F_{1,k} \sum_{k=1}^2 \left[ 2D_{27}^{1,k} + 4D_{312}^{1,k} - D_{12}^{1,k} \hat{s} - D_{24}^{1,k} \hat{s} - D_{26}^{1,k} \hat{s} - D_{310}^{1,k} \hat{s} - D_{26}^{1,k} \hat{t} - D_{38}^{1,k} \hat{t} \right. \\
& - D_{12}^{1,k} \hat{u} - D_{22}^{1,k} \hat{u} - D_{24}^{1,k} \hat{u} - D_{36}^{1,k} \hat{u} + 4D_{27}^{2,k} + 4D_{311}^{2,k} - D_{13}^{2,k} \hat{s} - D_{25}^{2,k} \hat{s} - D_{26}^{2,k} \hat{s} - D_{310}^{2,k} \hat{s} \\
& - D_{12}^{2,k} \hat{t} - 2D_{24}^{2,k} \hat{t} - D_{34}^{2,k} \hat{t} - D_{13}^{2,k} \hat{u} - 2D_{25}^{2,k} \hat{u} - D_{35}^{2,k} \hat{u} + 2D_{27}^{3,k} + 2D_{311}^{3,k} + (D_{12}^{1,k} \\
& + D_0^{2,k} + D_{11}^{2,k}) m_b^2 + (D_{24}^{1,k} - D_{22}^{1,k} + D_{26}^{1,k} - D_{32}^{1,k} + D_{36}^{1,k} + D_{38}^{1,k} + D_{13}^{2,k} \\
& \left. - D_0^{2,k} - 3D_{11}^{2,k} + D_{12}^{2,k} - 3D_{21}^{2,k} + 2D_{24}^{2,k} + 2D_{25}^{2,k} - D_{31}^{2,k} + D_{34}^{2,k} + D_{35}^{2,k}) m_{\tilde{\chi}_1^+}^2 \right] \\
f_{12}^{b,t} &= \frac{ig_s^2}{32\pi^2} \sum_{k=1}^2 F_{1,k} \left[ 2D_{27}^{1,k} + 2D_{312}^{1,k} + C_0^2 - 2D_{27}^{2,k} + 2D_{311}^{2,k} + D_{26}^{2,k} \hat{s} + D_{24}^{2,k} \hat{t} \right. \\
& \left. + D_{25}^{2,k} \hat{u} - 2D_{27}^{3,k} - 2D_{311}^{3,k} + (D_{21}^{2,k} - D_{24}^{2,k} - D_{25}^{2,k}) m_{\tilde{\chi}_1^+}^2 - D_0^{2,k} m_{t_k}^2 \right]
\end{aligned}$$

$$\begin{aligned}
f_{13}^{b,t} &= -\frac{ig_s^2}{16\pi^2} \sum_{k=1}^2 F_{1,k} \left[ D_{27}^{1,k} + D_{313}^{1,k} + D_{27}^{2,k} + D_{312}^{2,k} - D_{312}^{3,k} \right] \\
f_{14}^{b,t} &= \frac{ig_s^2}{16\pi^2} \sum_{k=1}^2 F_{1,k} \left[ D_{26}^{1,k} + D_{38}^{1,k} + D_{12}^{2,k} + 2D_{24}^{2,k} + D_{34}^{2,k} - D_{12}^{3,k} - 2D_{24}^{3,k} - D_{34}^{3,k} \right] \\
f_{15}^{b,t} &= -\frac{ig_s^2}{16\pi^2} \sum_{k=1}^2 F_{1,k} \left[ D_{27}^{1,k} + D_{311}^{1,k} + D_{313}^{2,k} - D_{313}^{3,k} \right] \\
f_{16}^{b,t} &= \frac{ig_s^2}{16\pi^2} \sum_{k=1}^2 F_{1,k} \left[ D_{12}^{1,k} + D_{22}^{1,k} + D_{24}^{1,k} + D_{36}^{1,k} + D_{13}^{2,k} + 2D_{25}^{2,k} + D_{35}^{2,k} \right. \\
&\quad \left. - D_{13}^{3,k} - 2D_{25}^{3,k} - D_{35}^{3,k} \right] \\
f_{17}^{b,t} &= f_{18}^{b,t} = -\frac{ig_s^2}{32\pi^2} \sum_{k=1}^2 \left[ (D_{12}^{1,k} + D_0^{2,k} + D_{11}^{2,k}) F_{2,k} m_b + (D_{12}^{1,k} + D_{22}^{1,k} + D_0^{2,k} + 2D_{11}^{2,k} \right. \\
&\quad \left. + D_{21}^{2,k}) F_{1,k} m_{\tilde{\chi}_1^+} \right] \\
f_{19}^{b,t} &= -f_{21}^{b,t} = -\frac{ig_s^2}{64\pi^2} \sum_{k=1}^2 F_{1,k} \left[ 2D_{27}^{1,k} + 4D_{27}^{2,k} + 6D_{312}^{2,k} - D_{26}^{2,k} \hat{s} - D_{38}^{2,k} \hat{s} - D_{12}^{2,k} \hat{t} \right. \\
&\quad \left. - D_{22}^{2,k} \hat{t} - D_{24}^{2,k} \hat{t} - D_{36}^{2,k} \hat{t} - D_{26}^{2,k} \hat{u} - D_{310}^{2,k} \hat{u} + D_{12}^{2,k} m_b^2 + (D_{22}^{2,k} - D_{24}^{2,k} + D_{26}^{2,k} \right. \\
&\quad \left. + D_{310}^{2,k} - D_{34}^{2,k} + D_{36}^{2,k}) m_{\tilde{\chi}_1^+}^2 \right] \\
f_{20}^{b,t} &= -f_{22}^{b,t} = \frac{ig_s^2}{32\pi^2} \sum_{k=1}^2 F_{1,k} \left[ D_{12}^{1,k} + D_{24}^{1,k} + D_{13}^{2,k} + D_{25}^{2,k} \right] \\
f_{23}^{b,t} &= f_{24}^{b,t} = -\frac{ig_s^2}{32\pi^2} \sum_{k=1}^2 \left[ (D_0^{2,k} + D_{11}^{2,k}) F_{2,k} m_b + (D_0^{2,k} + 2D_{11}^{2,k} + D_{21}^{2,k}) F_{1,k} m_{\tilde{\chi}_1^+} \right] \\
f_{25}^{b,t} &= -f_{27}^{b,t} = -\frac{ig_s^2}{64\pi^2} \sum_{k=1}^2 F_{1,k} \left[ 2D_{27}^{2,k} + 6D_{313}^{2,k} - D_{13}^{2,k} \hat{s} - D_{23}^{2,k} \hat{s} - D_{26}^{2,k} \hat{s} - D_{39}^{2,k} \hat{s} \right. \\
&\quad \left. - D_{12}^{2,k} \hat{t} - D_{13}^{2,k} \hat{t} - D_{24}^{2,k} \hat{t} - D_{25}^{2,k} \hat{t} - D_{26}^{2,k} \hat{t} - D_{310}^{2,k} \hat{t} - D_{13}^{2,k} \hat{u} - D_{23}^{2,k} \hat{u} - D_{25}^{2,k} \hat{u} - D_{37}^{2,k} \hat{u} \right. \\
&\quad \left. + (D_0^{2,k} + D_{13}^{2,k}) m_b^2 + (D_{37}^{2,k} - D_0^{2,k} - 2D_{11}^{2,k} + D_{12}^{2,k} + D_{13}^{2,k} - D_{21}^{2,k} + D_{23}^{2,k} + D_{24}^{2,k} \right. \\
&\quad \left. + D_{26}^{2,k} + D_{310}^{2,k} - D_{35}^{2,k}) m_{\tilde{\chi}_1^+}^2 \right] \\
f_{26}^{b,t} &= -f_{28}^{b,t} = -\frac{ig_s^2}{32\pi^2} \sum_{k=1}^2 F_{1,k} \left[ D_{12}^{2,k} + D_{24}^{2,k} \right] \\
f_{31}^{b,t} &= f_{32}^{b,t} = \frac{ig_s^2}{64\pi^2} \sum_{k=1}^2 \left[ (4D_{27}^{2,k} - D_{13}^{2,k} \hat{s} - D_{26}^{2,k} \hat{s} - D_0^{2,k} \hat{t} - D_{11}^{2,k} \hat{t} - D_{12}^{2,k} \hat{t} - D_{24}^{2,k} \hat{t} - D_{13}^{2,k} \hat{u} \right.
\end{aligned}$$

$$\begin{aligned}
& - D_{25}^{2,k} \hat{u}) F_{2,k} m_b + D_0^{2,k} F_{2,k} m_b^3 + (6D_{27}^{2,k} + 6D_{311}^{2,k} - D_{13}^{2,k} \hat{s} - D_{25}^{2,k} \hat{s} - D_{26}^{2,k} \hat{s} - D_{310}^{2,k} \hat{s} \\
& - D_0^{2,k} \hat{t} - 2D_{11}^{2,k} \hat{t} - D_{12}^{2,k} \hat{t} - D_{21}^{2,k} \hat{t} - 2D_{24}^{2,k} \hat{t} - D_{34}^{2,k} \hat{t} - D_{13}^{2,k} \hat{u} - 2D_{25}^{2,k} \hat{u} - D_{35}^{2,k} \hat{u} \\
& + D_0^{2,k} m_b^2 + D_{11}^{2,k} m_b^2) F_{1,k} m_{\tilde{\chi}_1^+} + (D_{12}^{2,k} - D_{11}^{2,k} + D_{13}^{2,k} - D_{21}^{2,k} + D_{24}^{2,k} + D_{25}^{2,k}) F_{2,k} m_b m_{\tilde{\chi}_1^+}^2 \\
& + (D_{12}^{2,k} - D_{11}^{2,k} + D_{13}^{2,k} - 2D_{21}^{2,k} + 2D_{24}^{2,k} + 2D_{25}^{2,k} - D_{31}^{2,k} + D_{34}^{2,k} + D_{35}^{2,k}) F_{1,k} m_{\tilde{\chi}_1^+}^3 \Big] \\
f_{33}^{b,t} &= f_{34}^{b,t} = -\frac{ig_s^2}{64\pi^2} \sum_{k=1}^2 \left[ D_0^{2,k} F_{2,k} m_b + (D_0^{2,k} + D_{11}^{2,k}) F_{1,k} m_{\tilde{\chi}_1^+} \right] \\
f_i^{b,t} &= 0 \quad (i = 29, 30, 35, 36)
\end{aligned}$$

In this work we adopted the definitions of two-, three-, and four-point one loop Passarino-Veltman integral functions as shown in Ref.[19] and all the vector and tensor integrals can be deduced in the forms of scalar integrals [20].

## References

- [1] H. E. Haber and G. L. Kane, Phys. Rep. **117**,75(1985).
- [2] S. Weinberg, Phys. Rev. D26(1982)287.
- [3] L.J. Hall and M. Suzuki, Nucl. Phys. B231(1984)419.
- [4] P. Roy, TIFR/TH/97-60; D.K. Ghosh, S. Raychaudhuri and K. Sridhar, Phys. Lett. B396(1997)177.
- [5] K. Agashe and M. Graesser, Phys. Rev. D54(1996)4445; J-H. Jiang, J.G. Kim and J.S. Lee, Phys. Rev. D55(1997)7296; Phys. Lett. B408(1997)367; Phys. Rev. D58(1998)035006.

- [6] G. Bhattacharyya, D. Choudhury and K. Sridhar, Phys. Lett. B355(1995)193; R. Barbier et.al, hep-ph/9810232.
- [7] D.K. Ghosh and S. Raychaudhuri, Phys. Lett. B422(1998)187.
- [8] G. Moreau, E. Perez and G. Polesello, 'Resonant sneutrino production in Supersymmetry with R-parity violation at the LHC', hep-ph/0003012.
- [9] M. Drees and S. P. Martin, hep-ph/9504324.
- [10] G. Farrar and P. Fayet, Phys. Lett, **B76**, 575(1978); Phys. Lett. **B79**, 442 (1978).
- [11] L. Ibanez and G. G. Ross, Phys. Lett. **B260** 291 (1991), Nucl. Phys. **B368** 3 (1992); J. Ellis, S. Lola and G. G. Ross, Nucl. Phys. **B526** 115 (1998).
- [12] J.F. Gunion and H.E. Haber, Nucl. Phys. **B272**,1(1986).
- [13] W.G. Ma, F. Du, M.L. Zhou et al, Phys. Rev.**D60**,115009 (1999).
- [14] Y. Jiang, W.G. Ma, L. Han, Z.H. Yu and H. Pietschmann, hep-ph/0003291, to appear in Phys. Rev. D.
- [15] A.D. Martin, W.J. Stirling and R.G. Roberts, Phys. Lett. **B354**, 155(1995).
- [16] B.C. Allanach, A. Dedes, H.K. Dreiner, Phys. Rev. **D60** 056002(1999).
- [17] V. Barger, M. S. Berger and P. Ohmann, Phys. Rev. **D47**, 1093(1993), **D47**, 2038(1993); V. Barger, M. S. Berger, P. Ohmann and R. J. N. Phillips, Phys. Lett. **B314**, 351(1993); V. Barger, M. S. berger and P. Ohmann, Phys. Rev. **D49**, 4908(1994).

[18] B. Allanach et. al, hep-ph/9906224.

[19] Bernd A. Kiehl, Phys. Rep. **240** 211(1994)

[20] G. Passarino and M. Veltman, Nucl. Phys. **B160**, 151(1979)

### Figure Captions

**Fig.1** The Feynman diagrams of the subprocess  $gg \rightarrow \tilde{\chi}_1^+ \mu^-$ . (a.1 ~ 3) box diagrams. (b.1) quartic interaction diagrams. (c.1) triangle diagrams.

**Fig.2** Total cross section of the process  $pp \rightarrow gg \rightarrow \tilde{\chi}_1^+ \mu^- + X$  as a function of  $m_{\tilde{\chi}_1^+}$  at the LHC with  $\sqrt{s} = 14 \text{ TeV}$ .

**Fig.3** Total cross section of the process  $pp \rightarrow gg \rightarrow \tilde{\chi}_1^+ \mu^- + X$  as a function of  $m_{\tilde{\nu}_\mu}$  at the LHC with  $\sqrt{s} = 14 \text{ TeV}$ .

**Fig.4** Total cross section of the process  $pp \rightarrow gg \rightarrow \tilde{\chi}_1^+ \mu^- + X$  as a function of  $\sqrt{s}$  at the LHC in the mSUGRA scenario.